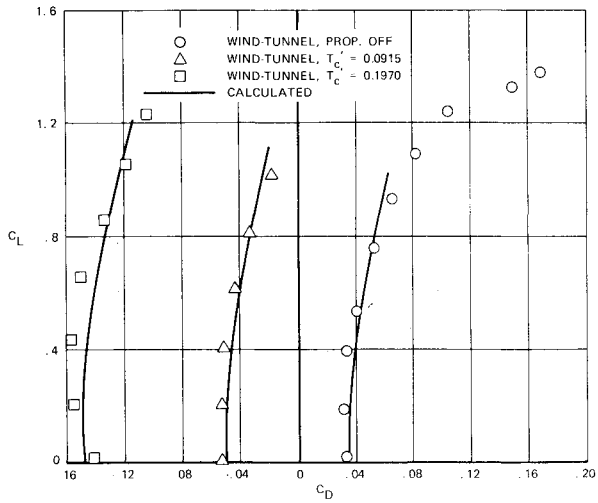

Fig. 2 Comparison of predicted drag with wind-tunnel data for different power conditions.

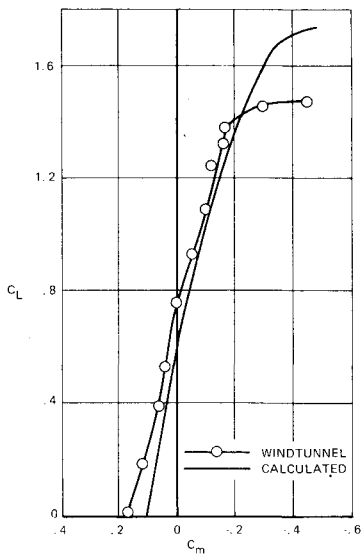

Fig. 3 Pitching moment of airplane; propellers removed and stabilizer not deflected.

from the experimental value. This is caused by the omission of the nacelle effect on C_{m0}.

The effects of power from propeller operation on lift, pitching moment, and drag were considered by the method presented in Ref. 4. In Fig. 2, the influence of power on drag is demonstrated. The effect of power on aerodynamic characteristics is well predicted by the method of Ref. 4. However, in the case of the ATLIT, opening of the engine inlets and engine cowl flaps has a considerable effect on airplane lift, pitching moment, and, especially, drag. The method used to predict power effects does not include engine cooling system effects. Changes in lift, pitching moment, and drag due to cooling system were derived from wind-tunnel data.

Conclusions

In Ref. 3, an analytical method is presented for predicting longitudinal aerodynamic characteristics of light, twin-engine, propeller driven airplanes. The method is applied to the ATLIT airplane and the calculated characteristics are compared with full-scale wind-tunnel data. The calculated lift-curve shows only fair agreement with the wind-tunnel results. Pitching moment and drag coefficient, however, are well predicted, as is the effect of power on the aerodynamic characteristics. No attempt was made to calculate the effects of engine cooling system, yet it does have a considerable effect on C_m and C_D.

Acknowledgment

This work was supported by NASA Langley Research Center under Grant NSG-1574.

References

[1] Holmes, B.J., "Flight Evaluation of an Advanced Technology Light Twin-Engine Airplane (ATLIT)," NASA CR-2832, July 1977.

[2] Hassell, J.L. Jr., Newsom, W.A. Jr., and Yip, L.P., "Full-Scale Wind-Tunnel Investigation of the Advanced Technology Light Twin-Engine Airplane (ATLIT)," NASA TP-1591, May 1980.

[3] van Dam, C.P., Griswold, M., and Roskam, J., "Comparison of Theoretical Predicted Longitudinal Aerodynamic Characteristics with Full-Scale Wind-Tunnel Data on the ATLIT Airplane," NASA CR-158753, July 1979.

[4] Wolowicz, C.H. and Yancey, R.B., "Longitudinal Aerodynamic Characteristics of Light, Twin-Engine, Propeller Driven Airplane," NASA TN D-6800, June 1972.

[5] Finck, R.D. and Hoak, D.E., "USAF Stability and Control DATCOM," Air Force Flight Dynamics Laboratory, Wright-Patterson Air Force Base, Ohio, Oct. 1960 (Revised Jan. 1975).

[6] Torenbeek, E., *Synthesis of Subsonic Airplane Design,* Delft University Press, Delft, Netherlands, 1976.

[7] Hess, J.L., "Calculation of Potential Flow about Arbitrary Three-Dimensional Lifting Bodies," MDC-J5679/01, NASC, Oct. 1972.

[8] Lan, C.E., "A Quasi Vortex Lattice Method in Thin Wing Theory," *Journal of Aircraft,* Vol. 11, Sept. 1974, pp. 518-527.

[9] McGhee, R.J. and Beasley, W.D., "Low-Speed Aerodynamic Characteristics of a 17-Percent Thick Airfoil Section Designed for General Aviation Applications," NASA TN D-7428, Dec. 1973.

[10] Smetana, F.O., "Comparison of Predicted with Measured Aerodynamic Characteristics of the ATLIT Airplane," SAE Paper 770449, Wichita, Kansas, March 1977.

AIAA 81-4187

Spanwise Lift Distribution of Forward- and Aft-Swept Wings in Comparison to the Optimum Distribution Form

G. Löbert*
Messerschmitt-Bölkow-Blohm GmbH, Munich, Federal Republic of Germany

Nomenclature

b	= wing span
c	= wing chord
$\bar{c}$	= mean wing chord
c_l	= local lift coefficient
C_D	= induced drag coefficient
C_L	= lift coefficient
D	= induced drag
f	= scale factor, see Eq. (1)
L	= lift
M	= freestream Mach number
M_B	= wing bending moment
s	= wing semispan
S, S_w	= wing area
t	= wing thickness
w	= weight function, see Eq. (2)
W_w	= wing weight
y	= spanwise distance from wing centerline
Λ_{LE}	= leading-edge sweep
η	= $2y/b$, nondimensional spanwise distance
$\tilde{\eta}$	= auxiliary spanwise coordinate, see Eq. (5)

Subscripts

1,2,3 = quantities pertaining to wings 1, 2, or 3

Received June 18, 1980; revision received Sept. 23, 1980.

*CCV Program Manager, Military Aircraft Division.

Introduction

EVER since the publication of Munk's dissertation on the optimum distribution of the lifting forces acting on one or more surfaces[1] it has been common practice to regard elliptical lift as the distribution form producing the least vortex drag on a monoplane wing. This result, however, is correct only if the span of the wing is kept constant. It is obvious that a different lift distribution and wing span will produce minimum vortex drag if the restriction on span is removed and a requirement with respect to wing weight is introduced instead. This Note describes a method of obtaining the optimum spanwise lift distribution for wings with a given weight. Additionally, the lift distributions of the aft-swept and the forward-swept plane trapezoidal wings are compared with this distribution form.

Analysis

Two wings of equal areas ($S_1 = S_2$), equal sweep angles, and equal relative thickness distributions $[t_1/c_1(\eta_1) = t_2/c_2(\eta_2)]$ producing equal lifts ($L_1 = L_2$) and having in general different spans ($b_1 \neq b_2$), different chord distributions $[c_1(\eta_1) \neq c_2(\eta_2)]$, different lift distributions $[b_1(\mathrm{d}L_1/\mathrm{d}y_1) \neq b_2(\mathrm{d}L_2/\mathrm{d}y_2)]$, and different vortex drags ($D_1 \neq D_2$) are given. In order to be able to compare the relative merits of the two wings, one of them must be transformed geometrically such that a common basis for performance comparison is obtained.

By increasing the span of wing 2 by a factor f and reducing the chords by the same factor, wing 3 is obtained. For this wing the following relations hold:

$$b_3 = fb_2 \tag{1a}$$

$$c_3(\eta_3) = c_2(\eta_2)/f \tag{1b}$$

$$t_3(\eta_3) = t_2(\eta_2)/f \tag{1c}$$

$$S_3 = S_2 = S_1 \tag{1d}$$

$$L_3 = L_2 = L_1 \tag{1e}$$

$$\mathrm{d}L_3/\mathrm{d}y_3 = (\mathrm{d}L_2/\mathrm{d}y_2)/f \tag{1f}$$

$$D_3 = D_2/f^2 \tag{1g}$$

The factor f follows from the requirement that the weights of wings 3 and 1 shall be the same. Considering that for simple beams the weight of the material needed to support the bending moments is proportional to

$$w \equiv \int_0^s \frac{M_B}{t}\,\mathrm{d}y \tag{2}$$

one can assume the weights of wings 3 and 1 to be approximately equal if $S_3 = S_1$ and $w_3 = w_1$. Since wing bending moment is proportional to Lb, Eq. (2) shows that

$$w_3 = w_2 \frac{f}{1/f} f = w_2 f^3 \tag{1h}$$

The condition $w_3 = w_1$ then leads to

$$f = (w_1/w_2)^{1/3} \tag{3}$$

Inserting Eq. (3) in Eq. (1g) one obtains

$$D_3 = D_2(w_2/w_1)^{2/3} \tag{4}$$

D_3 is the value with which the vortex drag of wing 1 has to be compared.

When determining the spanwise lift distribution for minimum vortex drag at constant lift and constant wing weight using nondimensional data, it is not C_D/C_L^2 but the expression

$$\frac{C_D}{C_L^2}\left[\int_0^1 \frac{\tilde{t}/s}{t(\eta)/s}\int_\eta^1 \frac{c_l(\tilde{\eta})c(\tilde{\eta})/s}{C_L\bar{c}/s}(\tilde{\eta}-\eta)\,\mathrm{d}\tilde{\eta}\,\mathrm{d}\eta\right]^{2/3} \tag{5}$$

that has to be minimized. Note that, in contrast to Ref. 4, the above analysis covers the important case of a nonconstant wing thickness $t(\eta)$.

Results

Using a simple parameter variation method, the spanwise distribution of lift that reduces Eq. (5) to a minimum was obtained for a linear thickness variation and a tip/root thickness ratio of 0.2. This is shown in Fig. 1 in comparison to the elliptical distribution of equal w. As can be seen, the optimum distribution has a lower loading on the outer wing and a correspondingly higher loading near the root. Due to the larger span, the wing with the nonelliptical distribution produces 5% less vortex drag than the wing with the elliptical form.

In Fig. 2 the constant-weight optimum lift distribution is compared with the lift distributions of two untwisted trapezoidal wings having an aspect ratio of 3.5, a taper ratio of 0.2, and leading-edge sweep angles of +30 and −30 deg, respectively. These loadings were calculated for $M = 0.8$ using the Weissinger[2] method. As can be seen, the spanwise loading of the plane forward-swept wing (FSW) is almost identical with the optimum distribution form, while that of the aft-swept wing (ASW) differs considerably. While both wings can

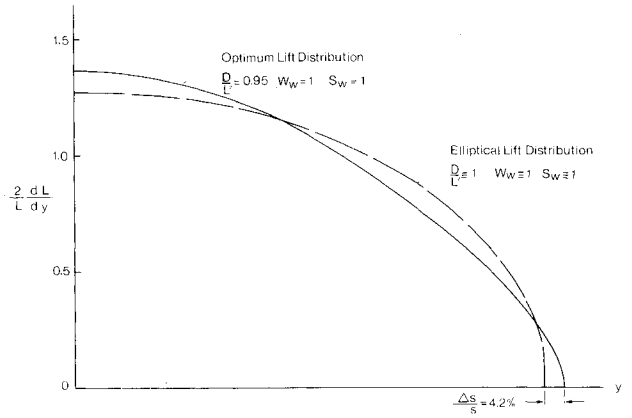

Fig. 1 Optimum lift distribution of constant-area, constant-weight wing in comparison to elliptical distribution form (tip/root thickness ratio = 0.2).

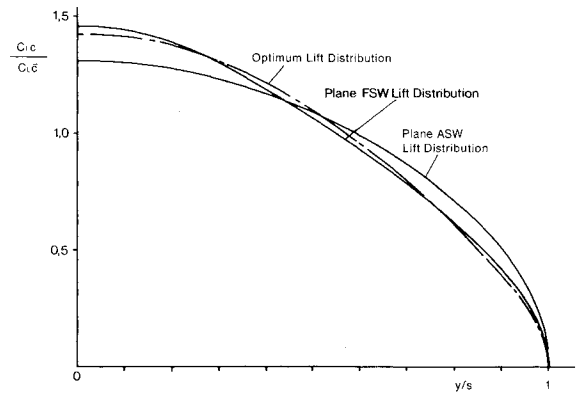

Fig. 2 Spanwise lift distribution of plane FSW ($\Lambda_{LE} = -30$ deg) and plane ASW ($\Lambda_{LE} = 30$ deg) in comparison with optimum distribution form (aspect ratio = 3.5, taper ratio = 0.2, $M = 0.8$).

be cambered and twisted in such a way that the desired lift distribution is obtained for a given speed, altitude, and load factor, the ASW requires a considerably larger amount of twist than the FSW. Consequently, the ASW will experience larger drag penalties in off-design conditions. Aeroelastic tailoring can, of course, alleviate this problem in that the elastic wash-out occurring on the ASW when lift is increased can partly compensate the corresponding aerodynamic wash-in. However, aerodynamic/elastic matching can be obtained at only one particular equivalent airspeed.

Conclusion

When vortex drag is minimized for a given wing weight a nonelliptical spanwise lift distribution form is obtained that shows reduced loading on the outer wing and correspondingly increased wing loading at the root. This distribution form produces 5% less vortex drag than the elliptical distribution. The forward-swept trapezoidal plane wing with a taper ratio of 0.2 and −30 deg leading-edge sweep has a lift distribution very close to the optimum distribution form, while the lift distribution of the corresponding aft-swept wing differs considerably from this. The ASW will, therefore, experience a higher deterioration of the spanwise lift distribution at off-design conditions. In contrast, an untwisted FSW fitted with an aeroisoclinic behavior[3] will exhibit an almost ideal lift distribution at all subsonic points of the flight envelope.

References

[1]Munk, M.M., "The Minimum Induced Drag of Aerofoils," NACA Rept. 121, 1921.

[2]Weißinger, J., "Über eine Erweiterung der Prandtlschen Theorie der tragenden Linie," *Mathematische, Nachrichten,* Vol. 2, Jan./Feb. 1949, pp. 45-106.

[3]Weisshaar, T.A., "Aeroelastic Tailoring of Forward Swept Wings," *Proceedings of 21st Structures, Structural Dynamics, and Materials Conference,* Seattle, Wash., May 12-14, 1980, pp. 761-770.

[4]Klein, A. and Viswanathan, S.P., "Approximate Solution for Minimum Induced Drag of Wings with Given Structural Weight," *Journal of Aircraft,* Vol. 12, Feb. 1975, pp. 124-126.

AIAA 81-4188

Dynamic Stress in a Towing Wire due to Forced Acceleration

C. Matuk*
University of Luleå, Luleå, Sweden

Introduction

WIRES used to tow bodies in air or water occasionally break. The reason is often a combination of static and dynamic stresses which causes the total stress to reach the tensile strength somewhere in a wire. The static stress is due to gravity and aerodynamic or hydrodynamic drag, and reaches its maximum at the towing end. The dynamic stress can be caused by accelerations of the towing vehicle. In this Note dynamic stress due to such accelerations is studied in the case of rectilinear motion (see Fig. 1).

The diameter of the wire is small compared to the wavelengths of the dominant Fourier components of the elastic waves. Also, internal friction in the wire is neglected. Thus, the one-dimensional wave equation applies. The towed body is represented by a rigid mass.

Received June 24, 1980; revision received March 9, 1981.

*Department of Mechanical Engineering.

Glauert[1] was one of the first who studied the shape of a towing wire. The case of a very light wire was investigated by Landweber and Protter.[2] The inclusion of wave propagation in towing came later, e.g., see Narkis.[3] Genin, Citron, and Huffman[4] considered dynamic stress caused by a variable force applied to the towed body.

Theory

Consider a towing vehicle which first travels at a constant velocity and then accelerates to a higher constant velocity. The towing wire is characterized by its density ρ, Young's modulus E, cross-sectional area A, and length L. The towed body is characterized by its mass m.

A reference frame moving with the original constant velocity of the towing vehicle is used. The longitudinal displacement in the wire is denoted by $u(x,t)$, where x is the position and t the time. Thus, the velocities appearing in this Note are velocities in excess of the original vehicle velocity. Also, the stress is dynamic stress in excess of the original static stress. The dynamic stress $\sigma = E\partial u/\partial x$ is related to the particle velocity $v = \partial u/\partial t$ by

$$\partial\sigma/\partial t = E\partial v/\partial x \tag{1}$$

The particle velocity satisfies the wave equation

$$\partial^2 v/\partial t^2 = c^2\partial^2 v/\partial x^2 \tag{2}$$

where $c = (E/\rho)^{1/2}$ is the elastic wave speed.

Initially, the wire is free from dynamic stress and at rest in the moving reference frame. Thus, the initial conditions are

$$\sigma(x,0) = 0, \quad v(x,0) = 0, \quad \partial v(x,0)/\partial t = 0, \quad 0 < x < L \tag{3}$$

The dynamic stress at the towed end is related to the velocity of the towed body through Newton's second law. Also, the velocity at the towing end is the same as the velocity v_T of the towing vehicle. Thus, the boundary conditions are

$$m\partial v(0,t)/\partial t = A\sigma(0,t), \quad v(L,t) = v_T(t), \quad t > 0 \tag{4}$$

The following dimensionless parameters are convenient to introduce here:

$$\xi = x/L, \quad \tau = t/T_0, \quad V = v/v_0, \quad V_T = v_T/v_0$$
$$\mu = m/M, \quad \lambda = T_0/t_0, \quad S = \sigma/\sigma_0 \tag{5}$$

where $T_0 = L/c$ is the transit time for a wave through the wire and $M = \rho AL$ is the mass of the wire. t_0 is the time during which the towing vehicle accelerates and v_0 is the final velocity increase. Also, $\sigma_0 = m(v_0/t_0)/A$ is defined as reference stress. μ can be interpreted as a dimensionless mass of the towed body and λ as a dimensionless length of the wire.

Equations (5) are used to make Eqs. (1-4) dimensionless. Laplace transformation [$\mathcal{L}\{f(\xi,\tau)\} = \tilde{f}(\xi,s)$] then gives

$$\mu\lambda s\tilde{S} = \partial\tilde{V}/\partial\xi \tag{6}$$

$$\partial^2\tilde{V}/\partial\xi^2 - s^2\tilde{V} = 0 \tag{7}$$

$$s\tilde{V}(0,s) = \lambda\tilde{S}(0,s), \quad \tilde{V}(1,s) = \tilde{V}_T(s) \tag{8}$$

The solution of Eqs. (6) and (7), with the boundary conditions in Eqs. (8), gives the Laplace transform $\tilde{S}$ of the dynamic